



James Dooley,^{1,2} Josselyn E. Garcia-Perez,^{1,2} Jayasree Sreenivasan,^{1,2,3}
 Susan M. Schlenner,^{1,2} Roman Vangoitsenhoven,⁴ Aikaterini S. Papadopoulou,^{1,5}
 Lei Tian,^{1,2} Susann Schonefeldt,^{1,2} Lutgarde Serneels,^{1,5} Christophe Deroose,⁶
 Kim A. Staats,^{1,2} Bart Van der Schueren,⁴ Bart De Strooper,^{1,5} Owen P. McGuinness,⁷
 Chantal Mathieu,⁴ and Adrian Liston^{1,2}



The microRNA-29 Family Dictates the Balance Between Homeostatic and Pathological Glucose Handling in Diabetes and Obesity

Diabetes 2016;65:53–61 | DOI: 10.2337/db15-0770

The microRNA-29 (miR-29) family is among the most abundantly expressed microRNA in the pancreas and liver. Here, we investigated the function of miR-29 in glucose regulation using miR-29a/b-1 (miR-29a)-deficient mice and newly generated miR-29b-2/c (miR-29c)-deficient mice. We observed multiple independent functions of the miR-29 family, which can be segregated into a hierarchical physiologic regulation of glucose handling. miR-29a, and not miR-29c, was observed to be a positive regulator of insulin secretion in vivo, with dysregulation of the exocytotic machinery sensitizing β -cells to overt diabetes after unfolded protein stress. By contrast, in the liver both miR-29a and miR-29c were important negative regulators of insulin signaling via phosphatidylinositol 3-kinase regulation. Global or hepatic insufficiency of miR-29 potently inhibited obesity and prevented the onset of diet-induced insulin resistance. These results demonstrate strong regulatory functions for the miR-29 family in obesity and diabetes, culminating in a hierarchical and dose-dependent effect on premature lethality.

The role of microRNA (miRNA) in glucose handling remains largely unknown; however, there are several a priori reasons to postulate an important function. Blood

glucose levels are subject to large environmental challenges due to dietary consumption. miRNA can act to stabilize stochastic perturbations, acting as a buffer against fluctuation in basal transcription and making it attractive to speculate that miRNA may have important functions in regulating glucose handling (1). Indeed, mutations in the miRNA-splicing enzyme Dicer have been associated with a number of endocrine disturbances (2), with severe effects of Dicer-deficiency on pancreatic β -cells (3–5) and hepatocytes (6,7). Many miRNA changes have been correlatively associated with defective glucose regulation (8,9); however, the physiological functions of few have been investigated.

The miRNA-29 (miR-29) family is among the most abundantly expressed miRNA in the pancreas and liver in mice and humans. The miR-29 family has been identified as a candidate regulator of glucose handling; however, the function of physiological in vivo expression has remained unstudied. The miR-29 family constitutes four species with identical seed sequences and is located in two genomic clusters, with miR-29a/b-1 in the *miR-29a* cluster and miR-29b-2/c in the *miR-29c* cluster (10). Here, through the generation of floxed and knockout mice, we identified the vital functions of the miR-29 family in the regulation of glucose metabolism. In contradiction to earlier in vitro

¹VIB, Leuven, Belgium

²Department of Microbiology and Immunology, KUL – University of Leuven, Leuven, Belgium

³Department of Oncology, KUL – University of Leuven, Leuven, Belgium

⁴Department of Clinical and Experimental Medicine, KUL – University of Leuven, Leuven, Belgium

⁵Center for Human Genetics, KUL – University of Leuven, Leuven, Belgium

⁶Department of Imaging and Pathology, KUL – University of Leuven, Leuven, Belgium

⁷Department of Molecular Physiology and Biophysics, Vanderbilt University, Nashville, TN

Corresponding author: James Dooley, james.dooley@vib-kuleuven.be, or Adrian Liston, adrian.liston@vib.be.

Received 5 June 2015 and accepted 5 October 2015.

This article contains Supplementary Data online at <http://diabetes.diabetesjournals.org/lookup/suppl/doi:10.2337/db15-0770/-/DC1>.

J.E.G.-P. and J.S. contributed equally as second authors.

© 2016 by the American Diabetes Association. Readers may use this article as long as the work is properly cited, the use is educational and not for profit, and the work is not altered.

experiments, miR-29a is a potent positive regulator of insulin secretion, required to prevent diabetes during unfolded protein stress of the β -cell. By contrast, the entire miR-29 family potentiates obesity and insulin resistance via hepatic regulatory functions.

RESULTS AND DISCUSSION

miR-29a is among the most abundant miRNA in pancreatic β -cells in mice and humans. In order to determine the *in vivo* function of miR-29a, we measured blood glucose levels of *miR-29a/b-1* knockout mice (11) (described here as *miR-29a*^{-/-} mice). Compared with wild-type siblings, *miR-29a*^{-/-} and *miR-29a*^{+/-} mice demonstrated higher fasting blood glucose (Fig. 1A) and reduced serum insulin (Fig. 1B). After glucose challenge, these effects were accentuated, with higher peak glucose after challenge (Fig. 1C) and sharply impaired serum insulin release (Fig. 1D). Serum IGF-1 was elevated, while sirtuin (SIRT) 1–4 expression remained normal (Supplementary Fig. 1). To comprehensively understand the role of the miR-29 family, we generated a knockout allele of the *miR-29b-2/c* locus, described here as *miR-29c*^{-/-} mice. As with miR-29a-deficient mice, *miR-29c*^{-/-} mice were born at normal ratios with no unusual histological abnormalities (data not shown). In contrast to *miR-29a*^{-/-} mice, *miR-29c*^{-/-} mice showed normal fasting blood glucose and insulin compared with wild-type siblings (Fig. 1E and F) and no glucose intolerance despite mildly impaired insulin secretion (Fig. 1G and H), demonstrating that the glucose intolerance phenotype was specific to the *miR-29a*^{-/-} strain.

To determine the mechanistic basis of the glucose intolerance phenotype, we assessed insulin levels in β -cells of *miR-29a*^{-/-} mice. The normal insulin protein and mRNA levels indicated that the defect was in insulin secretion rather than production (Fig. 1I–L). Likewise, *in vitro* glucose-stimulated insulin secretion assays demonstrated defected insulin secretion at baseline level, although this is corrected for under high glucose, indicating a differential *in vitro* consequence of miR-29a deficiency (Supplementary Fig. 3). Transplantation experiments, whereby *miR-29a*^{-/-} mice were transplanted with wild-type islets, rescued the fasting insulin levels and glucose intolerance (Fig. 1A–C), demonstrating an islet-intrinsic function. This positive regulatory role for miR-29a in insulin secretion *in vivo* was in direct contradiction to the previously described negative regulatory effect using cell lines *in vitro* (12). The negative effect of miR-29a on *in vitro* insulin release was proposed to be mediated by downregulation of Onecut2 (a validated miR-29a target) and the subsequent suppression of the insulin secretion-promoting protein granuphilin (9), while suppression of Mct1 (a validated miR-29a target [13]) is proposed to prevent exogenous pyruvate from triggering insulin (14,15). The expression changes in Onecut2 and granuphilin were not observed *in vivo* (data not shown), while that for Mct1 was observed (Fig. 1M), but the phenotype associated with increased Mct1 expression *in vitro*

was not observed *in vivo*. Of the negative regulators of insulin secretion, syntaxin-1a has been validated *in vitro* as a direct miR-29 target (16). In *miR-29a*^{-/-} islets, expression of *Stx1a* was increased 100% compared with wild-type levels (Fig. 1N), as was the mRNA encoding the related exocytotic protein Vamp3 (Fig. 1O), which is also a predicted miR-29a target. As 30% overexpression of *Stx1a* in islets is sufficient to cause hyperglycemia and reduced insulin secretion (17), this molecular interaction is sufficient to explain the *in vivo* phenotype observed.

The positive, rather than negative, function of miR-29a in insulin secretion necessitates a reinterpretation of the observation that miR-29a is upregulated in prediabetic NOD islets (9). Based on the *in vitro* negative regulatory role of miR-29a in glucose-stimulated insulin release (12), miR-29a upregulation was suggested to be a pathogenic event in type 1 diabetes (T1D), reducing insulin production (9). As our *in vivo* data were in polar opposition to the *in vitro* data, we tested the effect of miR-29a in diabetes development. We used a newly developed model for diabetes whereby the expression of the insHEL transgene causes subclinical unfolded protein stress in β -cells, a key contributor to T1D development. Unfolded protein stress in this model results in inefficient insulin processing, which is compensated for by increased secretion (J.D., J.E.G.-P., L.T., S.S., A.L., unpublished observations). On the wild-type background, no diabetes develops; however, the insHEL transgene results in diabetes in both *miR-29a*^{+/-} and *miR-29a*^{-/-} mice (Fig. 1P). These results demonstrate that miR-29a is actually protective during β -cell deficiency by enabling superior insulin secretion and suggest that the upregulation in prediabetic NOD islets is actually a compensatory protective mechanism to increase insulin secretion after reduction of β -cell mass.

During glucose challenge tests, *miR-29c*^{-/-} mice demonstrated normal glycemic control of the glucose challenge (Fig. 1G), while producing notably less additional insulin (Fig. 1H), suggesting an alteration of insulin sensitivity. To further investigate potential roles for the miR-29 family in insulin sensitivity, miR-29a- and miR-29c-deficient mice were tested for insulin tolerance. Wild-type mice, *miR-29a*^{-/-} mice, and *miR-29c*^{-/-} mice were fasted and challenged with exogenous insulin. Compared with wild-type mice, both *miR-29a*^{-/-} and *miR-29c*^{-/-} mice had an enhanced response to insulin, with a deeper and prolonged drop in blood glucose levels (Fig. 2A and B). The enhanced response to insulin in *miR-29a*^{-/-} mice was not corrected by islet transplantation (Fig. 2A), indicating that *miR-29a*^{-/-} mice have two distinct defects in glucose regulation: an islet-intrinsic defect in insulin secretion and an islet-extrinsic enhancement of insulin signaling. To test whether the effect was hepatic in origin, we generated *miR-29c*^{fl/fl} mice and crossed them to the Alb-Cre transgene, to induce liver-specific deficiency, with an 83% reduction at the tissue level (Fig. 2C). These mice also demonstrated enhanced responses to insulin, demonstrating a liver-specific component (Fig. 2D). Possible causes of this effect include

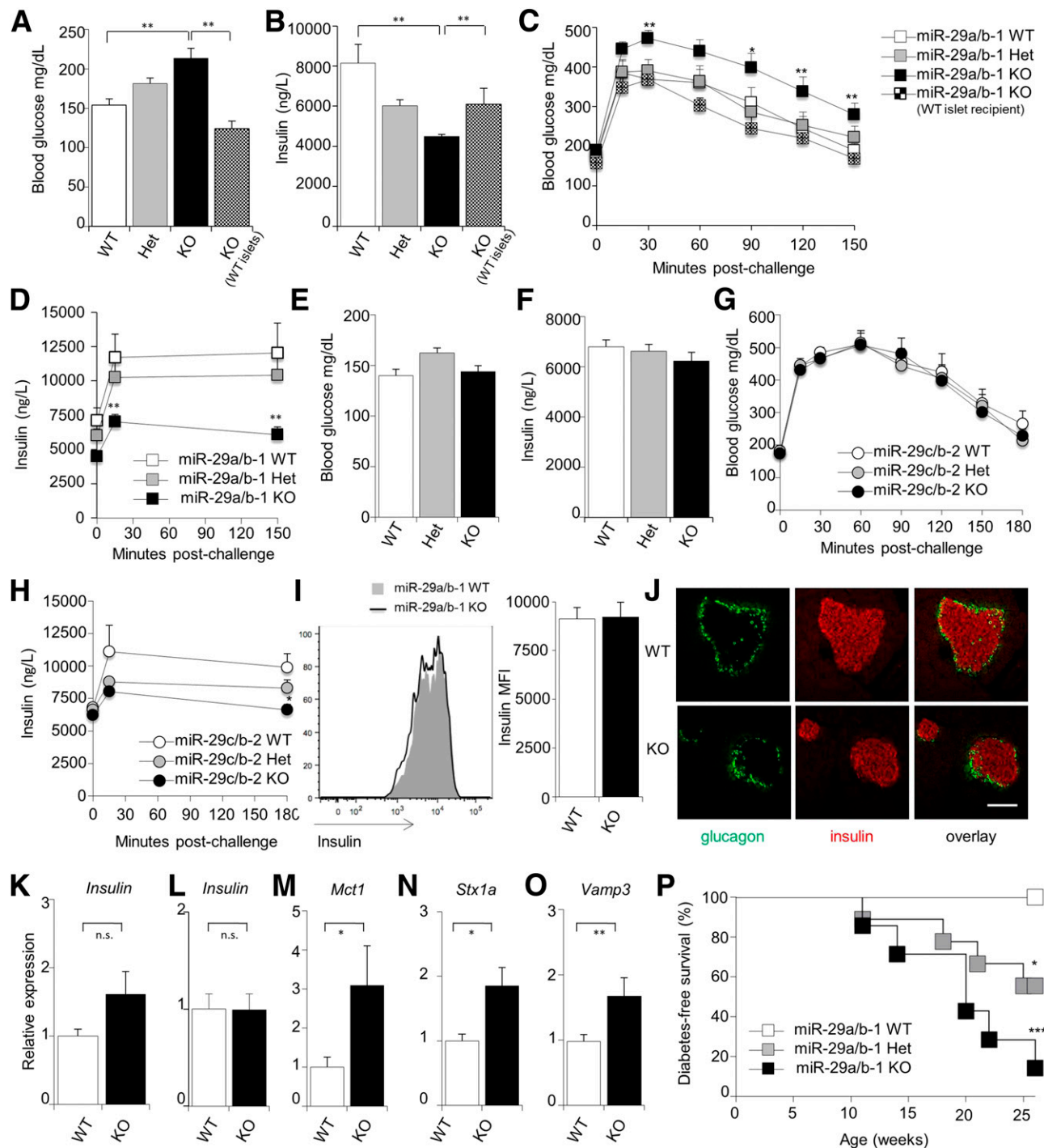


Figure 1—miR-29a prevents diabetes during unfolded protein stress by positive regulation of insulin secretion. **A–D**: Unmanipulated wild-type, *miR-29a*^{+/-}, and *miR-29a*^{-/-} mice, as well as *miR-29a*^{-/-} mice transplanted with wild-type islets, were fasted for 6 h. Fasting blood glucose levels (*n* = 19, 20, 19, and 5, respectively) (**A**) and fasting serum insulin levels (*n* = 16, 15, 9, and 6) (**B**). Blood glucose levels (*n* = 19, 20, 19, and 5) (**C**) and serum insulin levels (*n* = 16, 15, 9, and 6) (**D**) after glucose challenge. **E–H**: Wild-type, *miR-29c*^{+/-}, and *miR-29c*^{-/-} mice were fasted for 6 h. Fasting blood glucose levels (*n* = 9, 13, and 7) (**E**) and serum insulin levels (*n* = 9, 13, and 7) (**F**). Blood glucose levels (*n* = 9, 13, and 7) (**G**) and serum insulin levels (*n* = 9, 13, and 7) (**H**) after glucose challenge. **I**: Representative histograms and mean fluorescence intensity (MFI) of anti-insulin antibody staining on islets purified from wild-type and *miR-29a*^{-/-} mice (*n* = 5 and 4). **J**: Representative immunofluorescence staining on the pancreas of wild-type and *miR-29a*^{-/-} mice for insulin (red) and glucagon (green) (*n* = 3 and 4). Scale bar indicates 50 μm. **K**: Whole pancreas was taken from wild-type and *miR-29a*^{-/-} mice, and quantitative PCR was performed for *insulin* relative to *Rpl37a*. **L–O**: Islets were purified from wild-type and *miR-29a*^{-/-} mice, and quantitative PCR was performed for *insulin* (**L**), *Mct1* (**M**), *Stx1a* (**N**), and *Vamp3* (**O**) relative to *Rpl37a* (*n* = 7, 4). **P**: Diabetes incidence of insHEL transgenic males on the *miR-29a*^{wt/wt} (*n* = 11), *miR-29a*^{wt/0} (*n* = 9), and *miR-29a*^{0/0} (*n* = 7) backgrounds. No diabetes was observed in mice of any genotype without the insHEL transgene. Median ± SEM. **P* < 0.05, ***P* < 0.01, ****P* < 0.001. Het, heterozygote; KO, knockout; WT, wild-type.

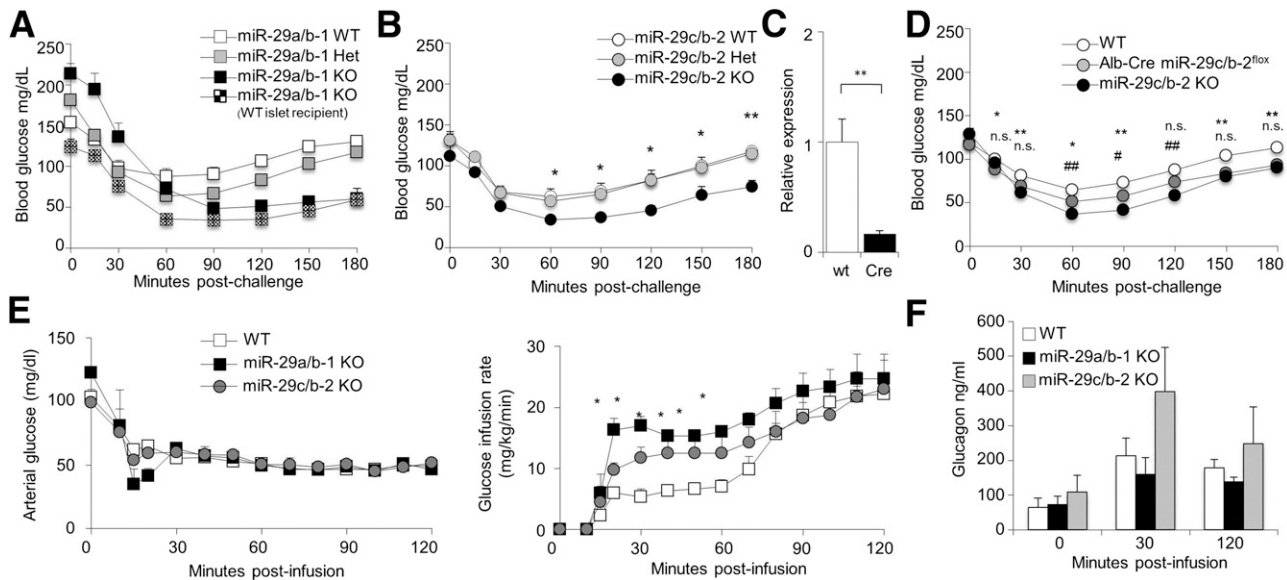


Figure 2—The miR-29 family is a positive regulator of insulin sensitivity in hepatocytes. *A*: Unmanipulated wild-type, *miR-29a*^{+/-}, and *miR-29a*^{-/-} mice, as well as *miR-29a*^{-/-} mice transplanted with wild-type islets, were fasted for 6 h and challenged with exogenous insulin prior to measurement of blood glucose levels (*n* = 24, 35, 19, and 6, respectively). *B*: Wild-type, *miR-29c*^{+/-}, and *miR-29c*^{-/-} mice were fasted for 6 h and challenged with exogenous insulin prior to measurement of blood glucose levels (*n* = 9, 13, and 7). *C*: Whole liver was taken from wild-type and Alb-Cre *miR-29c*^{fl/fl} mice (*n* = 6 and 6). Quantitative PCR was performed for *miR-29c* relative to *Sno202*. *D*: Wild-type, *miR-29c*^{-/-}, and Alb-Cre *miR-29c*^{fl/fl} mice were fasted for 6 h and challenged with exogenous insulin prior to measurement of blood glucose levels (*n* = 15, 5, and 8). * and # indicate significance of Alb-Cre *miR-29c*^{fl/fl} mice vs. wild-type and *miR-29c*^{-/-} mice, respectively. *E*: Wild-type, *miR-29a*^{-/-}, and *miR-29c*^{-/-} mice were challenged with hyperinsulinemic clamps and maintained at hypoglycemic blood glucose levels (left). The glucose infusion rate required to maintain stable hypoglycemia was calculated (right) (*n* = 7, 3, and 4). *F*: Glucagon levels from wild-type, *miR-29a*^{-/-}, and *miR-29c*^{-/-} mice during hypoglycemic-hyperinsulinemic clamps (*n* = 7, 3, and 4). Median ± SEM. **P* < 0.05, ***P* < 0.01, #*P* < 0.05, and ##*P* < 0.01. KO, knockout; WT, wild-type.

increased sensitivity to insulin or decreased effective counterregulatory response (impaired glucagon secretion). To control for insulin sensitivity, we performed hyperinsulinemic-hypoglycemic clamps on wild-type mice, *miR-29a*^{-/-} mice, and *miR-29c*^{-/-} mice. For maintenance of the same level of hypoglycemia during insulin infusion, both *miR-29a*^{-/-} and *miR-29c*^{-/-} mice required significantly greater glucose infusion (Fig. 2E), despite a robust α -cell response (Fig. 2F), indicating a shared hepatic role for the miR-29 family in inhibiting insulin activity.

A proposed explanation for elevated responses to insulin in miR-29-deficient mice would be defective gluconeogenesis. Forced in vivo overexpression studies previously demonstrated the miR-29 family to be a negative regulator of gluconeogenesis via the suppression of PGC-1 α and glucose-6-phosphatase (G6Pase) (18). However, expression of these genes was not significantly modified in *miR-29a*^{-/-} or *miR-29c*^{-/-} mice (Fig. 3A and B), and regardless, the direction of the published effect is incompatible with the observed phenotype. It is therefore likely that the previously observed suppression of PGC-1 α and G6Pase is due to off-target effects of overexpression rather than reflecting a function of physiological levels of expression. Further evidence against defective gluconeogenesis include the following: a normal increase in blood glucose after injection of exogenous glucagon in *miR-29a*^{-/-} mice (Fig. 3C), normal glucagon levels in pancreatic α -cells

in *miR-29a*^{-/-} mice (Figs. 1J and 3D), normal glucagon response to hypoglycemia, and no correction after islet transplantation (Fig. 2A). These results suggested that rather than gluconeogenesis being defective in miR-29-deficient mice, insulin signaling was prolonged, as observed in vitro with 3T3-L1 (19) and HepG2 (20) cells. This in vitro effect has been attributed to dysregulation of phosphatidylinositol 3-kinase (PI3K) (20), an effect observed in both *miR-29a*^{-/-} and *miR-29c*^{-/-} mice at both the mRNA and protein level (Fig. 3E and F). To formally test the role of PI3K in insulin hyperresponsiveness, we used the PI3K-inhibitor wortmannin. As wortmannin inhibits PI3K activity, treatment with wortmannin allows the truncation of insulin signaling at a defined time. Concurrent treatment with insulin and wortmannin inhibited hypoglycemia in both wild-type and *miR-29a*^{-/-} mice (Fig. 3G), demonstrating that hypoglycemia in insulin-treated *miR-29a*^{-/-} mice is dependent on classical PI3K-dependent insulin signaling. To determine whether the prolonged hypoglycemia observed in insulin-challenged *miR-29a*^{-/-} mice was due to continued PI3K signaling, we started wortmannin treatment at 60 min postinsulin injection, the time point at which wild-type mice reach the hypoglycemic trough. This treatment of *miR-29a*^{-/-} mice prevented the prolonged hypoglycemia normally observed, correcting blood glucose to that of wild-type levels (Fig. 3H). Together, these results demonstrate

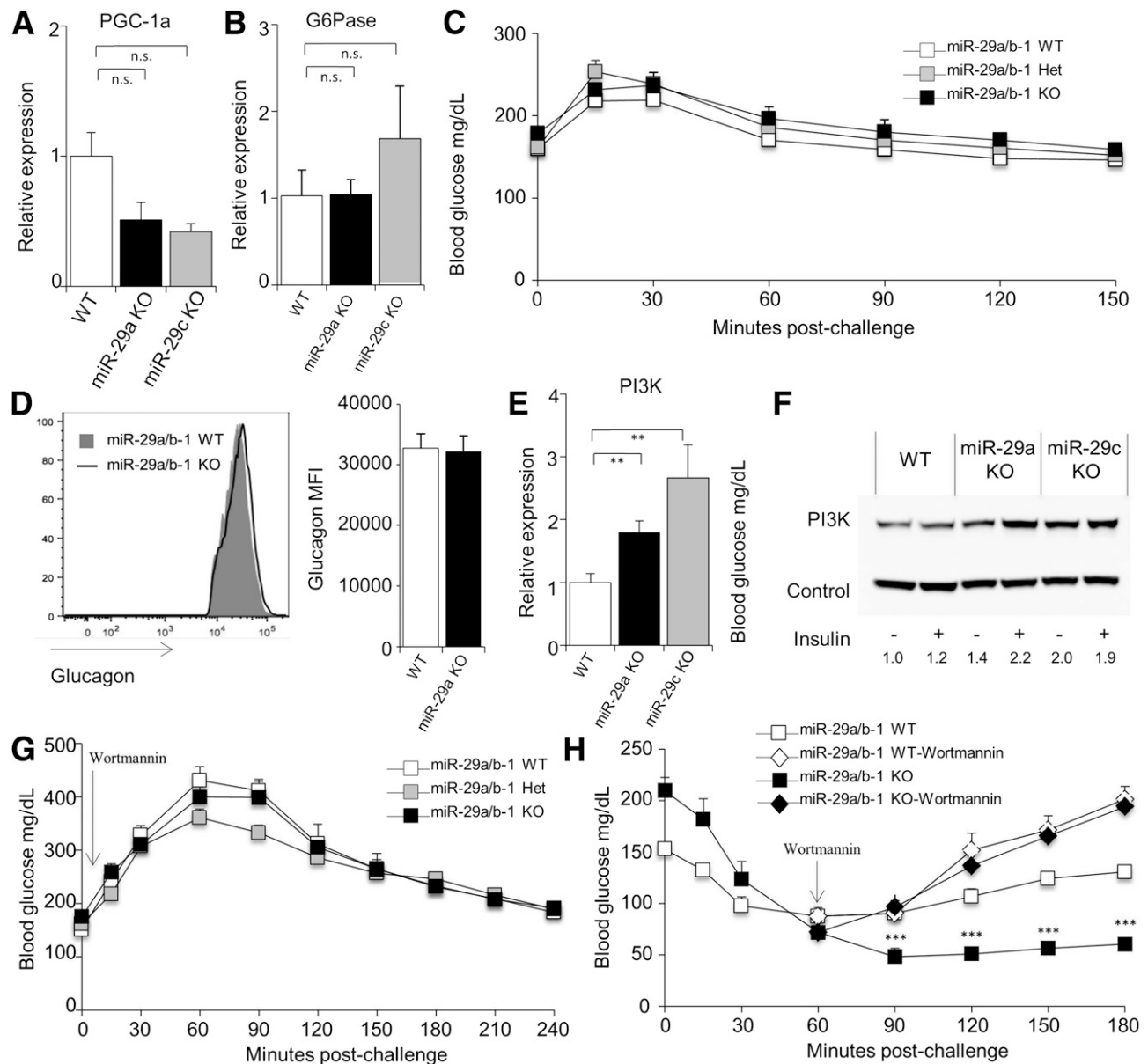


Figure 3—The miR-29 family regulates hepatic PI3K expression. cDNA was produced from the liver of wild-type, *miR-29a*^{-/-}, and *miR-29c*^{-/-} mice, and quantitative PCR was performed for *PGC-1a* (A) and *G6Pase* (B), relative to *Rpl37a* ($n = 9, 7, \text{ and } 3$, respectively). C: Blood glucose levels of wild-type, *miR-29a*^{+/-}, and *miR-29a*^{-/-} mice after fasting and challenge with exogenous glucagon. D: Mean fluorescence intensity (MFI) of anti-glucagon antibody staining on islets purified from wild-type and *miR-29a*^{-/-} mice ($n = 5 \text{ and } 4$). E: cDNA was produced from the liver of wild-type, *miR-29a*^{-/-}, and *miR-29c*^{-/-} mice, and quantitative PCR was performed for *PI3K*, relative to *Rpl37a* ($n = 9, 7, \text{ and } 3$). F: Protein lysate was produced from the liver of wild-type, *miR-29a*^{-/-}, and *miR-29c*^{-/-} mice after fasting at 30 min after insulin injection, and Western blotting was performed for PI3K. G: Wild-type, *miR-29a*^{+/-}, and *miR-29a*^{-/-} mice were fasted for 6 h, injected with wortmannin, and challenged with exogenous insulin, prior to measurement of blood glucose levels ($n = 4, 12, \text{ and } 6$). H: Wild-type and *miR-29a*^{-/-} mice were fasted for 6 h and challenged with exogenous insulin prior to measurement of blood glucose levels ($n = 28 \text{ and } 24$). At 60 min postinsulin treatment, wortmannin was given to a subset of individuals from each genotype ($n = 4 \text{ and } 6$). Median \pm SEM. ** $P < 0.01$ and *** $P < 0.001$. KO, knockout; n.s., not significant; WT, wild-type.

that elevated responses to insulin in miR-29-deficient mice are caused by prolonged insulin signaling due to elevated PI3K activity. It is notable that the prolonged insulin signaling did not impact fasting blood glucose levels, which were normal in *miR-29c*^{-/-} mice and in islet-transplanted *miR-29a*^{-/-} mice (correcting the insulin secretion defect), and only impacted glycemic control after

the insulin spike caused by glucose challenge. In a disease context, miR-29 expression is elevated in the liver of type 2 diabetic (T2D) mice (20), and thus may constitute a pathogenic process in disease by truncating the duration of insulin signaling.

To determine whether increased miR-29 expression could play a pathogenic role in T2D, despite the protective

role we found in a T1D-like context, we investigated the role of this family in diet-induced obesity and insulin resistance. At the macroscopic level, *miR-29a*^{-/-} mice had a 10% reduction in body weight (Fig. 4A), with a similar decrease in total length (Fig. 4B), while *miR-29c*^{-/-} mice had normal weights (Supplementary Fig. 4). Body composition analysis demonstrated that the diminished weight was due to a 50% reduction in white adipose tissue, with lean body mass intact (Fig. 4C and D and Supplementary Fig. 5) and circulating leptin significantly reduced (Fig. 4E). Studies performed in the 3T3-L1 adipocyte cell line suggested that miR-29a suppressed peroxisome proliferator-activated receptor δ (21); however, this was not observed in vivo (Supplementary Fig. 5D). Liver staining with Oil Red O indicated no compensatory hepatic accumulation of lipids (Supplementary Fig. 5E), and energy expenditure was not increased (Supplementary Fig. 6).

Rather, the reduction in adipose expansion was accompanied by reduced food intake (Fig. 4F), despite normal ghrelin levels (Fig. 4G). To simulate the processes of T2D, we placed the *miR-29a*^{-/-} mice and *miR-29c*^{-/-} mice on a high-fat diet. Unlike wild-type mice, which rapidly gained weight and became obese, both the *miR-29a*^{-/-} mice and *miR-29c*^{-/-} mice remained lean on the high-fat diet (Fig. 4H). We therefore placed Alb-Cre *miR-29c*^{fl/fl} mice on a high-fat diet and found that they also remained lean, demonstrating a liver-specific function of miR-29c in promoting diet-induced obesity. As *miR-29a*^{-/-} mice have conflicting effects of defective insulin secretion and enhanced insulin signaling, we restricted further analysis of the T2D process to *miR-29c*^{-/-} mice (which have no insulin secretion defect). Analysis of the response to insulin in high-fat diet-fed mice demonstrated insulin resistance in wild-type mice (Fig. 4I), a key hallmark of T2D

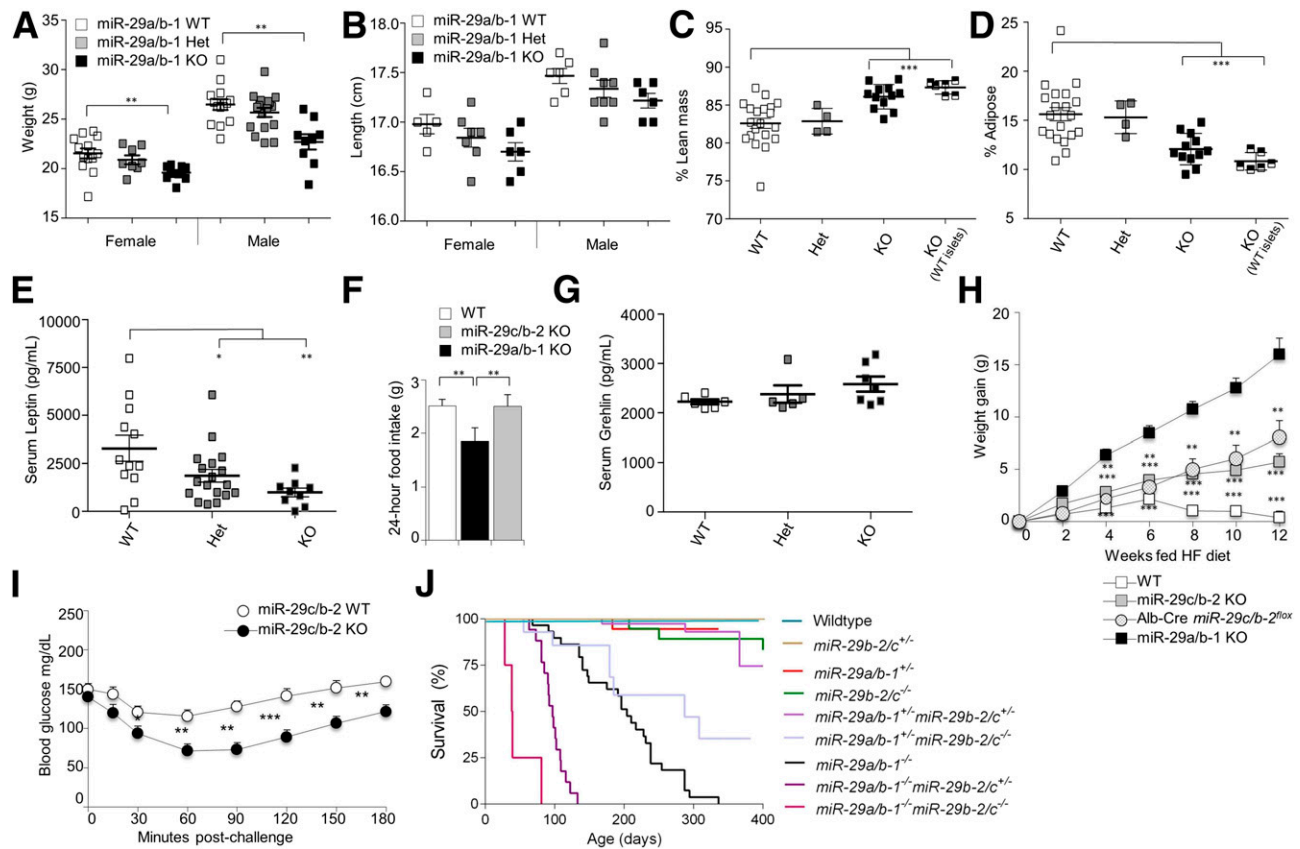


Figure 4—Loss of miR-29 family members protects against obesity and insulin resistance. Weights (A) and head-tail lengths (B) of wild-type, *miR-29a*^{-/-}, and *miR-29c*^{-/-} mice at 10 weeks of age, separated by sex (weights, $n = 13, 8,$ and $11,$ respectively, for female and $n = 14, 17,$ and 9 for male; length, $n = 5, 7,$ and 6 for female and $n = 6, 8,$ and 6 for male). Percentage body composition of lean mass (C) and adipose tissue mass (D) for unmanipulated wild-type, *miR-29a*^{+/-}, and *miR-29a*^{-/-} mice and *miR-29a*^{-/-} mice transplanted with wild-type islets, all at 14 weeks of age ($n = 20, 3, 12,$ and 5). E: Serum leptin concentrations in wild-type, *miR-29a*^{+/-}, and *miR-29a*^{-/-} mice at 10 weeks of age ($n = 12, 18,$ and 9). F: Food consumption for wild-type, *miR-29a*^{+/-}, and *miR-29c*^{-/-} mice at 10 weeks of age ($n = 8, 4,$ and 8). G: Serum total ghrelin concentrations in wild-type, *miR-29a*^{+/-}, and *miR-29a*^{-/-} mice at 10 weeks of age ($n = 6, 5,$ and 7). H: Weight gain for wild-type, *miR-29a*^{-/-}, *miR-29c*^{-/-}, and Alb-Cre *miR-29c*^{fl/fl} mice placed on a high-fat diet ($n = 32, 8, 13,$ and 6). I: Wild-type and *miR-29c*^{-/-} mice on a high-fat diet were fasted for 6 h and challenged with exogenous insulin prior to measurement of blood glucose levels ($n = 22$ and 13). J: Survival curve for wild-type, *miR-29a*^{+/-}, *miR-29a*^{-/-}, *miR-29c*^{+/-}, *miR-29c*^{-/-}, *miR-29a*^{+/-}*miR-29c*^{+/-}, *miR-29a*^{-/-}*miR-29c*^{+/-}, *miR-29c*^{+/-}*miR-29c*^{-/-}, and *miR-29a*^{-/-}*miR-29c*^{-/-} mice ($n = 29, 29, 29, 54, 24, 52, 17, 17,$ and 4). Median \pm SEM. * $P < 0.05,$ ** $P < 0.01,$ *** $P < 0.001.$

progression. However, high-fat-fed *miR-29c*^{-/-} mice did not develop insulin resistance, with a normal glycemic response to insulin challenge (Fig. 4I), indicating that the hepatic hypersensitivity to insulin is able to counter the progression of insulin desensitization in T2D. Glucose tolerance tests gave results consistent with those observed in low-fat conditions (Supplementary Fig. 7). These surprising results demonstrated the janus function of the miR-29 family in diabetes, with a protective role in β -cells and a pathogenic function in the liver.

Finally, with the full characterization of the individual strains, we intercrossed these two strains to generate quad-deficient mice, in which *miR-29a/b-1/b-2/c* were knocked out (named here as *miR-29a*^{-/-}*miR-29c*^{-/-} mice). Despite the lack of overt pathology in either parental strain, *miR-29a*^{-/-}*miR-29c*^{-/-} mice died at ~4 weeks of age (Fig. 4J). Survival analysis of partial miR-29-deficient demonstrated a hierarchical and dose-dependent synergistic effect. miR-29a was the more potent survival factor, with miR-29a-deficient mice dying at 7 months, while miR-29c-deficient mice showed little survival defect (Fig. 4J). The loss of a single copy at either miR-29 locus caused no survival defect; however, heterozygous loss in one locus synergized with deficiency in the other locus (Fig. 4J). Due to logistical and ethical constraints, it was not possible to examine the glucose regulation in *miR-29a*^{-/-}*miR-29c*^{-/-} mice; however, the early mortality indicates the synergistic importance of this miR family.

Through the analysis of *miR-29a*^{-/-} mice and the generation and analysis of *miR-29c*^{lox} and *miR-29c*^{-/-} mice, we have identified opposing functions of the miR-29 family in glucose metabolism. Involvement in several of these processes has been previously suggested in in vitro studies; however, in vivo analysis has revealed surprising role reversals and segregations in functions between family members. The critical functions include the following: 1) a positive regulatory role in insulin secretion by β -cells, which protects against forms of diabetes caused by β -cell deficiency (e.g., T1D); 2) a hepatic regulatory role in truncating the duration of insulin signaling, which sensitizes to T2D; and 3) a positive regulatory role in appetite and adiposity. The net effect of these multiple functions is a hierarchical and dose-dependent synergy of miR-29 deficiency in mortality. This result is a surprisingly severe effect compared with the relatively subtle phenotype of most other published miRNA knockouts (22) and suggests a nonlinear effect of increasingly disturbed glucose handling.

RESEARCH DESIGN AND METHODS

Mice

miR-29a knockout mice (11) and Alb-Cre mice (23) were used on the C57BL/6 background. insHEL mice (24) were on a mixed BL/6.BL.10 background. *miR-29c* floxed and knockout mice were generated as described in the Supplementary Data. Islet transplants were performed at 6 weeks under sterile conditions by isolating islets from 2- to 3-week-old wild-type mice (as described below),

and 150 islets were transplanted under the kidney capsule. Diabetes was tested for biweekly by blood glucose. Mice were diagnosed as diabetic when blood glucose exceeded 260 mg/dL after 2–3 h fasting for two sequential tests. Food consumption, physical activity, and energy expenditure was measured using TSE Systems Metabolic cages. Mice were housed under specific pathogen-free conditions, were fed using R/M-H ssniff chow or EF R/M with 30% fat ssniff chow, and were used in accordance with the KUL–University of Leuven Animal Ethics Committee, with the exception of the hypoglycemic clamps, which were approved by the Vanderbilt University Animal Care and Use Committee.

Glucose, Insulin, and Glucagon Challenges

Prior to challenge, mice were fasted for 6 h, blood glucose was measured, and a serum sample was collected. For the glucose tolerance test, mice were injected with 2 mg/g i.p. glucose in 0.9% NaCl. For the insulin tolerance test, mice were injected with 1.0 unit/kg i.p. human insulin (Actrapid, Novo Nordisk). For the glucagon tolerance test, mice were injected with 16 μ g/kg i.p. glucagon HCL (Novo Nordisk). After challenge, blood glucose was measured from the tail using ACCU-CHEK Aviva blood glucose strips at the indicated time points. Additional serum samples were collected for assessment of insulin concentrations (described below). For PI3K inhibition, mice were injected with 1.4 mg/kg i.p. wortmannin (Sigma) in 0.9% NaCl.

Hyperinsulinemic-Hypoglycemic Clamp

Catheters were implanted into a carotid artery and a jugular vein of mice for sampling and infusions, respectively, 5 days before the hyperinsulinemic-hypoglycemic clamps were performed on mice fasted for 5 h. Arterial glucose was clamped at 50 mg/dL using a variable rate of glucose infusion, which was adjusted based on the measurement of blood glucose at 10-min intervals. Baseline blood or plasma variables were obtained in blood samples collected at –5 min. At time zero, insulin infusion (10 mU/kg body wt/min) was started and continued for 120 min. Mice received heparinized saline-washed erythrocytes from donors at 5 μ L/min to prevent a fall in hematocrit. Glucagon levels were measured at $t = 0, 30,$ and 120 min by ELISA.

Glucose-Stimulated Insulin Secretion Assay

Islets were isolated from pancreas as previously described (25). Pancreata were digested by 0.8 mg/mL collagenase NB 8 (Serva) digestion at 37°C, and then islets were isolated through density gradient centrifugation with Dextran T70 (Pharmacosmos A/S) solution and handpicked under a dissection microscope. Pancreatic islets of 10- to 12-week-old mice were incubated in 10% RPMI 1640 with 5 mmol/L and 25 mmol/L glucose using a previously described protocol (26).

Serum Analysis

Serum samples were collected by retro-orbital bleed and were stored at –80°C. Total ghrelin levels were measured using a Mouse Ghrelin (total) ELISA kit by Millipore

according to manufacturer's instructions. Serum leptin concentrations were measured by ELISA (Mouse Leptin DuoSet, R&D Systems) as per the manufacturer's instructions. Insulin concentrations in serum and glucose-stimulated insulin secretion supernatant were measured by ELISA (cat. no. 10-1247-01; mouse insulin ELISA, Mercodia), as per the manufacturer's instructions. HbA_{1c} was measured using a Mouse Hemoglobin A1c kit for the quantitative determination of HbA_{1c} in mouse whole blood from Crystal Chem per the manufacturer's instructions. Serum IGF-1 concentrations were measured by ELISA (Mouse IGF-1, R&D Systems) per the manufacturer's instructions.

Expression Analysis

Islets were isolated from pancreas after the protocol described earlier (25). Total RNA was isolated from pancreatic islets and dissected white adipose tissue and liver using the RNeasy mini kit (Qiagen). cDNA was produced using the GoScript Reverse Transcription system (Promega) according to the manufacturer's protocol. Quantitative RT-PCR for mRNA was performed on a StepOnePlus Real-Time PCR machine (ABI) based on the SYBR green I fluorescence (FastSYBR Green Master Mix [ABI]) and analyzed by the $2^{-\Delta\Delta CT}$ method. Expression of miRNA was performed using TaqMan assays for snoRNA202 (identification no. 001232), mmu-miR-29a (identification no. 002447), and mmu-miR-29c (identification no. 001818). All mRNA values are normalized to *Rpl37a*, and miR values are normalized to snoRNA202.

For protein analysis, livers were lysed in radioimmunoprecipitation assay buffer in the presence of Lysing Matrix D (MP Biomedicals, Solon, OH) under vigorous shaking and then cleared by centrifugation, and protein content was measured using the Qubit fluorometer (Invitrogen, Carlsbad, CA). Gels were run and blotted using the NuPage electrophoresis system according to the manufacturer's recommendations (Invitrogen). The p85 subunit for PI3K was stained using the 4257 antibody (Cell Signaling, Danvers, MA). Mouse IgG heavy chain was used as loading control and stained using horseradish peroxidase-conjugated goat anti-mouse antibody (cat. no. 31430, Pierce, Rockford, IL).

Flow Cytometry

Flow cytometry was performed on pancreatic islet cells fixed and permeabilized with the Foxp3 staining kit (eBioscience) and stained with anti-insulin APC (clone 182410, R&D Systems) and anti-glucagon PerCP-Cy5.5 (clone 199017, R&D Systems) labeled using the Lightning-Link labeling kit (Innova Biosciences). Data were acquired on a FACSCanto II (BD) and analyzed with FlowJo software (Tree Star).

Imaging

Body composition was analyzed in vivo by DEXA (PIXImus densitometer, Lunar, Madison, WI), with software version 2.10.041. Mice were anesthetized with 0.05 mg/g i.p. pentobarbital.

Histology was performed on 4% paraformaldehyde-fixed tissues after hematoxylin-eosin staining. Assessment

of histological changes was performed by BioGenetics (Greenbank, WA). For lipid assessment, fresh frozen sections were fixed in 4% PFA and stained with Oil Red O. For immunofluorescence, pancreas sections were fresh frozen in optimal cutting temperature compound and stained according to manufacturer's protocol. Sections were stained using the monoclonal antibodies glucagon (FL-180; Santa Cruz), insulin A (C-12; Santa Cruz), and Glut2 (H-67; Santa Cruz). For immunofluorescence, the following detection antibodies were used: donkey anti-rabbit 488 and donkey anti-goat 546 (both from Molecular Probes). Images were acquired using a Zeiss LSM 510 metaconfocal microscope.

Statistics

Statistical analysis was performed using Prism (Graph-Pad). A significance threshold of 5% using ANOVA followed by individual *t* test comparisons was maintained throughout the study. Differences in survival rates were analyzed using a log-rank test (Prism).

Acknowledgments. The authors thank Diana Pombal, Willem Van den Bergh, and Yulia Lampi (KUL – University of Leuven) for technical assistance and Stephanie Humblet-Baron (KUL) for advice.

Funding. This work was supported by VIB and the Research Foundation Flanders (FWO). Hyperinsulinemic-hypoglycemic clamps were performed by the Vanderbilt Mouse Metabolic Phenotyping Center (DK-059637). B.V.d.S. was supported by the European Research Council (ERC), the Queen Elizabeth Foundation, and a Methusalem grant of the KUL–University of Leuven/Flemish Government. O.P.M. was supported by the National Institutes of Health (DK-59637, DK-020593, DK-078188, DK-043748). A.L. is supported by a JDRF Australia Career Development Award.

Duality of Interest. No potential conflicts of interest relevant to this article were reported.

Author Contributions. J.D., O.P.M., C.M., and A.L. designed the study. J.D., J.E.G.-P., J.S., S.M.S., R.V., L.T., S.S., K.A.S., and B.V.d.S. performed the experiments. A.S.P., L.S., and B.D.S. generated *miR-29c* mice. J.D. and A.L. wrote the manuscript. All authors discussed results and read and approved the manuscript. A.L. is the guarantor of this work and, as such, had full access to all the data in the study and takes responsibility for the integrity of the data and the accuracy of the data analysis.

References

- Rottiers V, Näär AM. MicroRNAs in metabolism and metabolic disorders. *Nat Rev Mol Cell Biol* 2012;13:239–250
- Choong CS, Priest JR, Foulkes WD. Exploring the endocrine manifestations of DICER1 mutations. *Trends Mol Med* 2012;18:503–505
- Mandelbaum AD, Melkman-Zehavi T, Oren R, et al. Dysregulation of Dicer1 in beta cells impairs islet architecture and glucose metabolism. *Exp Diabetes Res* 2012;2012:470302
- Kalis M, Bolmeson C, Esguerra JL, et al. Beta-cell specific deletion of Dicer1 leads to defective insulin secretion and diabetes mellitus. *PLoS One* 2011;6:e29166
- Melkman-Zehavi T, Oren R, Kredon-Russo S, et al. miRNAs control insulin content in pancreatic β -cells via downregulation of transcriptional repressors. *EMBO J* 2011;30:835–845
- Sekine S, Ogawa R, Mcmanus MT, Kanai Y, Hebrok M. Dicer is required for proper liver zonation. *J Pathol* 2009;219:365–372
- Sekine S, Ogawa R, Ito R, et al. Disruption of Dicer1 induces dysregulated fetal gene expression and promotes hepatocarcinogenesis. *Gastroenterology* 2009;136:2304–2315.e1–4

8. van de Bunt M, Gaulton KJ, Parts L, et al. The miRNA profile of human pancreatic islets and beta-cells and relationship to type 2 diabetes pathogenesis. *PLoS One* 2013;8:e55272
9. Roggli E, Gattesco S, Caille D, et al. Changes in microRNA expression contribute to pancreatic β -cell dysfunction in prediabetic NOD mice. *Diabetes* 2012;61:1742–1751
10. Liston A, Papadopoulou AS, Danso-Abeam D, Dooley J. MicroRNA-29 in the adaptive immune system: setting the threshold. *Cell Mol Life Sci* 2012;69:3533–3541
11. Papadopoulou AS, Dooley J, Linterman MA, et al. The thymic epithelial microRNA network elevates the threshold for infection-associated thymic involution via miR-29a mediated suppression of the IFN- α receptor. *Nat Immunol* 2012;13:181–187
12. Bagge A, Clausen TR, Larsen S, et al. MicroRNA-29a is up-regulated in beta-cells by glucose and decreases glucose-stimulated insulin secretion. *Biochem Biophys Res Commun* 2012;426:266–272
13. Pullen TJ, da Silva Xavier G, Kelsey G, Rutter GA. miR-29a and miR-29b contribute to pancreatic beta-cell-specific silencing of monocarboxylate transporter 1 (Mct1). *Mol Cell Biol* 2011;31:3182–3194
14. Ishihara H, Wang H, Drewes LR, Wollheim CB. Overexpression of monocarboxylate transporter and lactate dehydrogenase alters insulin secretory responses to pyruvate and lactate in beta cells. *J Clin Invest* 1999;104:1621–1629
15. Pullen TJ, Sylow L, Sun G, Halestrap AP, Richter EA, Rutter GA. Overexpression of monocarboxylate transporter-1 (SLC16A1) in mouse pancreatic β -cells leads to relative hyperinsulinism during exercise. *Diabetes* 2012;61:1719–1725
16. Bagge A, Dahmcke CM, Dalgaard LT. Syntaxin-1a is a direct target of miR-29a in insulin-producing β -cells. *Horm Metab Res* 2013;45:463–466
17. Lam PP, Leung YM, Sheu L, et al. Transgenic mouse overexpressing syntaxin-1A as a diabetes model. *Diabetes* 2005;54:2744–2754
18. Liang J, Liu C, Qiao A, et al. MicroRNA-29a-c decrease fasting blood glucose levels by negatively regulating hepatic gluconeogenesis. *J Hepatol* 2013;58:535–542
19. He A, Zhu L, Gupta N, Chang Y, Fang F. Overexpression of micro ribonucleic acid 29, highly up-regulated in diabetic rats, leads to insulin resistance in 3T3-L1 adipocytes. *Mol Endocrinol* 2007;21:2785–2794
20. Pandey AK, Verma G, Vig S, Srivastava S, Srivastava AK, Datta M. miR-29a levels are elevated in the db/db mice liver and its overexpression leads to attenuation of insulin action on PEPCK gene expression in HepG2 cells. *Mol Cell Endocrinol* 2011;332:125–133
21. Bouvy-Liivrand M, Heinäniemi M, John E, Schneider JG, Sauter T, Sinkkonen L. Combinatorial regulation of lipoprotein lipase by microRNAs during mouse adipogenesis. *RNA Biol* 2014;11:76–91
22. Park CY, Choi YS, McManus MT. Analysis of microRNA knockouts in mice. *Hum Mol Genet* 2010;19:R169–R175
23. Postic C, Shiota M, Niswender KD, et al. Dual roles for glucokinase in glucose homeostasis as determined by liver and pancreatic beta cell-specific gene knock-outs using Cre recombinase. *J Biol Chem* 1999;274:305–315
24. Akkaraju S, Ho WY, Leong D, Cnaan K, Davis MM, Goodnow CC. A range of CD4 T cell tolerance: partial inactivation to organ-specific antigen allows non-destructive thyroiditis or insulinitis. *Immunity* 1997;7:255–271
25. Li DS, Yuan YH, Tu HJ, Liang QL, Dai LJ. A protocol for islet isolation from mouse pancreas. *Nat Protoc* 2009;4:1649–1652
26. Gysemans CA, Ladrière L, Callewaert H, et al. Disruption of the gamma-interferon signaling pathway at the level of signal transducer and activator of transcription-1 prevents immune destruction of beta-cells. *Diabetes* 2005;54:2396–2403